Nuclear Instruments and Methods in Physics Research A 638 (2011) 83–91

Contents lists available at ScienceDirect

Nuclear Instruments and Methods in Physics Research A

journal homepage: www.elsevier.com/locate/nima

Development of a large-area monolithic 4 × 4 MPPC array for a future PET scanner employing pixelized Ce:LYSO and Pr:LuAG crystals

T. Kato [a,*], J. Kataoka [a], T. Nakamori [a], T. Miura [a], H. Matsuda [a], K. Sato [b], Y. Ishikawa [b], K. Yamamura [b], N. Kawabata [b], H. Ikeda [c], G. Sato [c], K. Kamada [d]

[a] Research Institute for Science and Engineering, Waseda University, 3-4-1, Ohkubo, Shinjuku, Tokyo, Japan
[b] Solid State Division, Hamamatsu Photonics K. K., 1126-1, Ichino-cho, Hamamatsu, Shizuoka, Japan
[c] ISAS/JAXA, 3-1-1, Yoshinodai, Chuo-ku, Sagamihara-shi, Kanagawa, Japan
[d] Materials Research Laboratory, Furukawa Co., Ltd., 1-25-13, Kannondai, Tsukuba, Ibaraki 305-0856, Japan

ARTICLE INFO

Article history:
Received 24 December 2010
Received in revised form
4 February 2011
Accepted 14 February 2011
Available online 26 February 2011

Keywords:
Multi-Pixel Photon Counter
Gamma-rays
Positron emission tomography

ABSTRACT

We have developed a new type of large-area monolithic Multi-Pixel Photon Counter (MPPC) array consisting of a 4 × 4 matrix of 3 × 3 mm^2 pixels. Each pixel comprises 3600 Geiger mode avalanche photodiodes (APDs) that achieve an average gain of 9.68 × 10^5 at 71.9 V at 0 °C with variations of only ± 7.2% over 4 × 4 pixels. Excellent uniformity was also obtained for photon detection efficiencies (PDE) of ± 6.4%, whilst dark count rates at the single photoelectron (1 p.e.) level amounted to ≃ 2 Mcps/pixel, measured at 0 °C. As the first step toward using the device in scintillation photon detectors, we fabricated a prototype gamma-ray camera consisting of an MPPC array optically coupled with a scintillator matrix, namely a 4 × 4 array of 3 × 3 × 10 mm^3 crystals. Specifically, we tested the performance with Ce-doped (Lu, Y)$_2$(SiO$_4$)O (Ce:LYSO), Pr-doped Lu$_3$Al$_5$O$_{12}$ (Pr:LuAG) and "surface coated" Pr:LuAG (Pr:LuAG (WLS)) matrices whereby the emission peak of Pr:LuAG was shifted from 310 to 420 nm via a wavelength shifter (WLS). Average energy resolutions of 13.83%, 14.70% and 13.96% (FWHM) were obtained for 662 keV gamma-rays, as measured at 0 °C with Ce:LYSO, Pr:LuAG and Pr:LuAG (WLS) scintillator matrices, respectively. We confirmed that the effective PDE for Pr:LuAG (WLS) had improved by more than 30% compared to original, non-coated Pr:LuAG matrix. These results suggest that a large-area monolithic MPPC array developed here could be promising for future medical imaging, particularly in positron emission tomography (PET).

1. Introduction

Positron emission tomography (PET) imaging is a well-established method for detecting cancers and diagnosing Alzheimer's in its early stages [1]. Currently, the PET combined with CT (CT-PET) has become more common as a multimodality imaging device [2], as it provides an improved insight into the spatial and temporal interrelations between functional and anatomical images. However, CT imaging suffers from poor soft-tissue contrast with patients also subjected to a significant radiation dose that exceeds that received from the PET itself. Magnetic Resonance Imaging (MRI), however, offers excellent soft-tissue contrast and anatomical detail without the additional radiation. Many advantageous aspects of MRI-PET are now being proposed, and testing of their prototypes is underway [3–5]. Unfortunately, the Photo-Multiplier Tube (PMT) incorporated in conventional PET scanners is difficult to use within the MRI high magnetic field. Moreover, the spatial resolution attainable with a PMT-based PET is far from the theoretical limit of PET resolution. Various PET modules utilizing an avalanche photodiode (APD) have successfully demonstrated the potential for simultaneous MRI-PET imaging [6] as well as ultimate sub-millimeter spatial resolutions [7]. One disadvantage of using APDs is, however, the relatively low

Table 1
Specification of the 4 × 4 MPPC array at +25 °C.

Parameters	Specification
Number of elements [ch]	16 (4 × 4)
Active area/channel (mm^2)	3 × 3
Pixel size of a Geiger-mode APD (μm)	50
Typical photon detection efficiency[1] (λ = 440 nm) (%)	50
Terminal capacitance/channel (pF)	320
Operation voltage (V)	73.0 ± 0.12
Gain	7.5 × 10^5
Typical dark current / channel (μA)	3

[1] Including cross-talk and after-pulse contributions.

* Corresponding author.
E-mail address: katou.frme.8180@asagi.waseda.jp (T. Kato).

0168-9002/$ - see front matter © 2011 Elsevier B.V. All rights reserved.
doi:10.1016/j.nima.2011.02.049

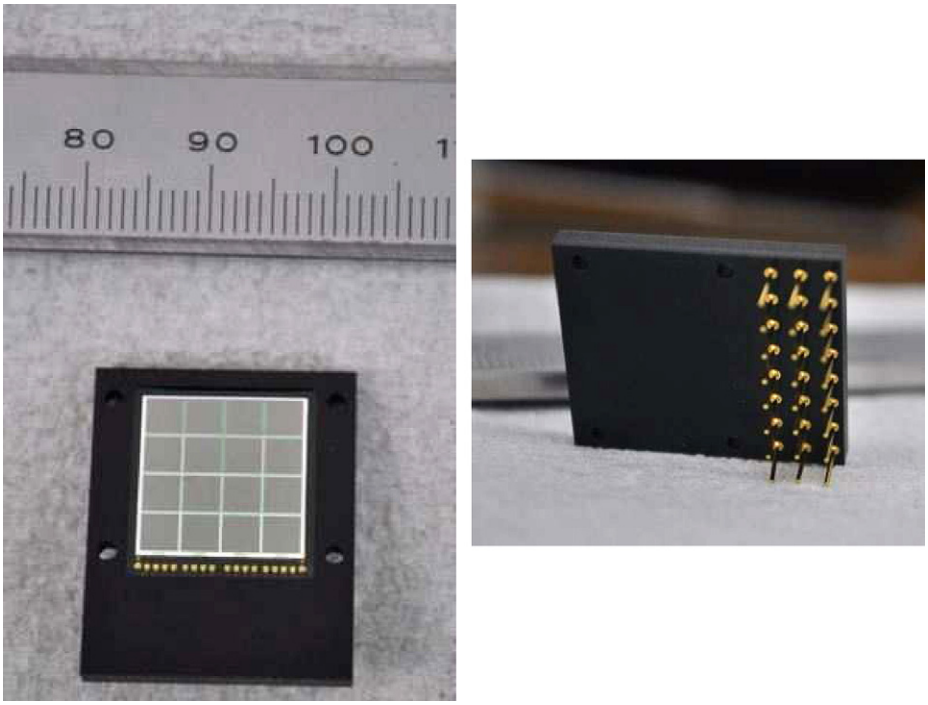

Fig. 1. Pictures of the 4×4 MPPC array developed in this paper.

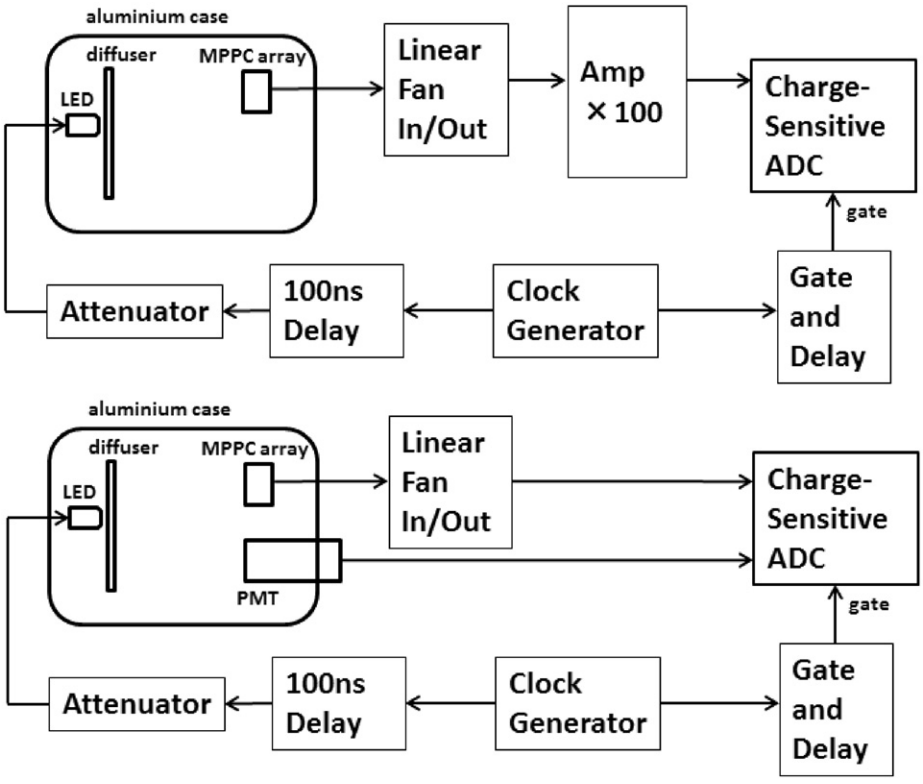

Fig. 2. Diagram of the readout system used for measuring the gain (*top*) and the proportionality (*bottom*).

avalanche gain (typically ≤ 100), meaning it is easily affected by electric noise contamination.

MPPC, also known as a Silicon Photo-Multiplier (SiPM), is a compact, high performance semiconductor photodetector consisting of multiple Geiger-mode APD pixels. Its operating principles and basic performance are summarized in Ref. [8]. The MPPC has many advantages like APDs described above, such as insensitivity to magnetic fields, effective time resolution and compactness. In addition, it is operated in Geiger-mode, meaning its gain may be almost comparable to that of PMTs at up to the 10^5-10^6 level. Despite its superior advantages, however, it also has several weak points compared to traditional PMTs and APDs. First, the

dynamic range of the MPPC is limited by the number of Geiger-mode APD pixels comprised in the device. Each of the latter is subject to dead time (typically measured in tens of ns) once the Geiger-discharge has triggered, during which multiple photons entering a single pixel cannot be counted, resulting in a non-linear response to the number of incident photons. Second, thermal electrons also trigger a Geiger-discharge, resulting in substantial contamination of dark counts, typically amounting to 3 Mcps for $3 \times 3\ mm^2$ MPPCs (whose Geiger-mode APDs are arranged with a pitch of 50 μm) measured at +25 °C [9]. Nevertheless, its great advantages make MPPC one of the ideal photosensors for MRI-PET and also for Time Of Flight (TOF) applications [10–13].

There is also a wide-ranging choice of scintillators to be used in the PET scanner, such as $Bi_{12}Ge_3O_{20}$ (BGO), Ce-doped $Gd_2(SiO_4)O$ (Ce:GSO), Ce-doped $Lu_2(SiO_4)O$ (Ce:LSO) and Ce-doped $(Lu, Y)_2(SiO_4)O$ (Ce:LYSO). In modern PET scanners, BGO is no longer used due to its low light yield (15% of Tl:NaI) and long scintillation

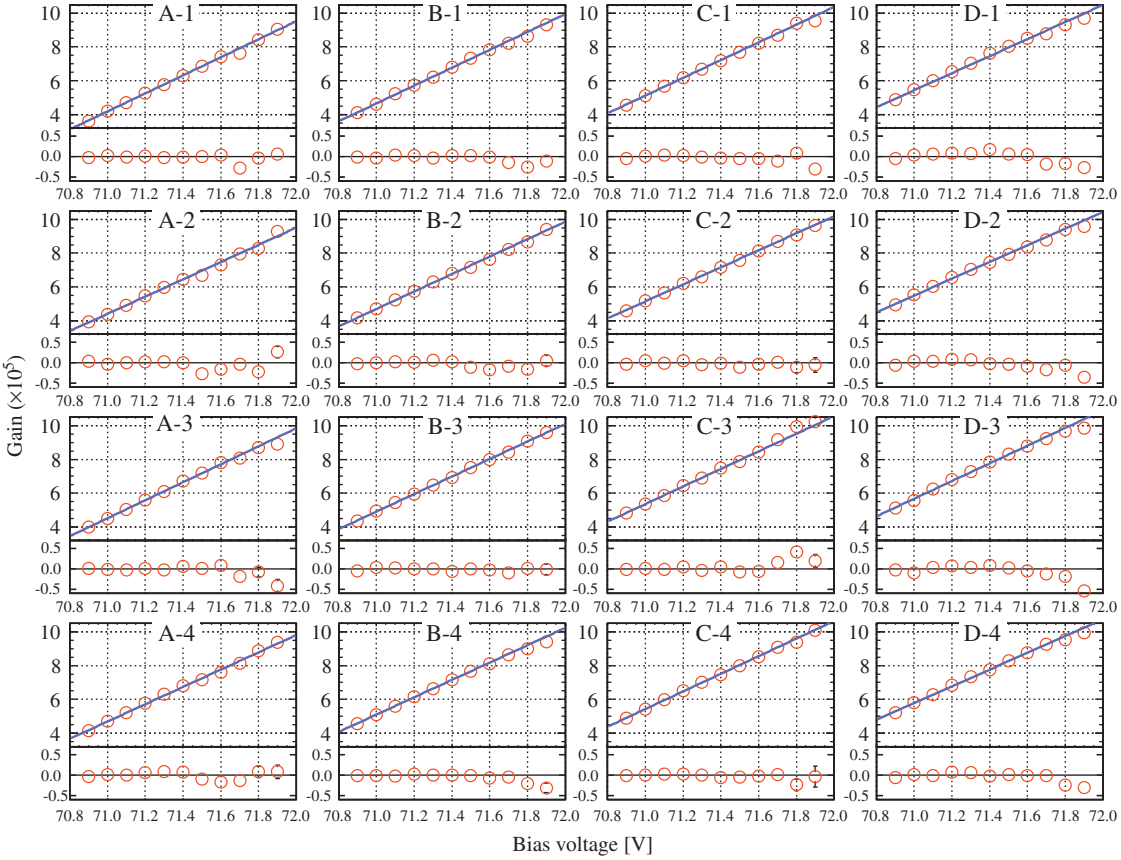

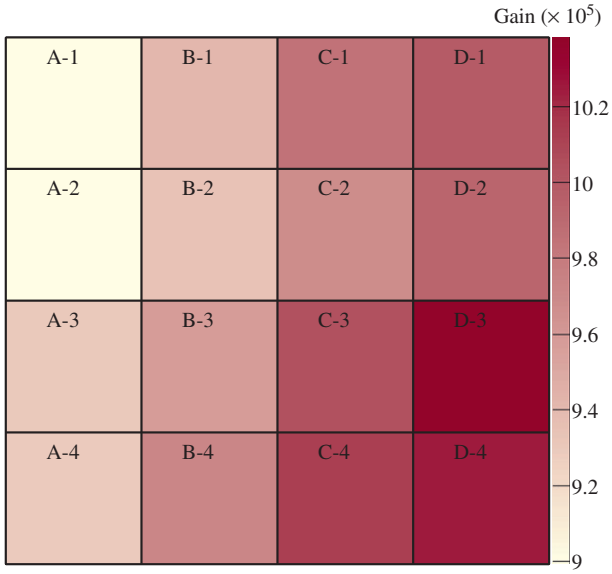

Fig. 3. *Top*: gain variation as a function of bias voltage for all pixels from 70.9 to 71.9 V, measured at 0 °C. In the top panel, circles and lines represent the actual measured value and the fitting line, respectively. The bottom panel shows the residual of the fitting line. *Bottom*: gain distribution at 71.9 V at 0 °C.

decay time (300 ns). The most popular scintillator at present is Ce:LSO or Ce:LYSO [14], both of which feature high light yield (75% of Tl:NaI), short scintillation decay time (40 ns) and high density (7.4 g/cm^3) greater than BGO (7.1 g/cm^3). Alternatively, brand-new scintillators with high light output and/or fast timing properties are being tested, especially for future applications in TOF-PET scanners. Pr-doped $Lu_3Al_5O_{12}$ (Pr:LuAG) is one such scintillator characterized by a very fast decay time (20 ns) and good light yield (53% of Tl:NaI) [15,16]. Since its light emission is sharply concentrated at around 310 nm, UV-enhanced APD arrays have been specifically developed to read out the Pr:LuAG scintillators [17].

Currently, the development of a high-resolution MRI-PET/TOF-PET technique utilizing the newly designed MPPC array is underway. As the first step, we report in this paper on the development of a large-area, monolithic 4×4 MPPC array and its performance as a gamma-ray detector coupled with Ce:LYSO and Pr:LuAG matrices. The advantage of using MPPC monolithic arrays, instead of single MPPC devices assembled together [18], is that we can easily achieve good uniformity of gain, PDE and dark counts over the pixels. Moreover, the gap between each pixel can be minimized, thereby improving the effective area of the MPPC arrays as a whole. Since the MPPC developed here is expected to be less sensitive to scintillation light at around 310 nm, we also fabricated a sample of a Pr:LuAG matrix, the surface of which was coated with an appropriate wavelength shifter (WLS).

This paper is organized as follows. In Section 2, we present the basic characteristics of a large-area monolithic 4×4 MPPC array developed in this paper. In Section 3, performances with various pixelized scintillator arrays will be given as a probe of the compact gamma-ray imager. The final conclusions are presented in Section 4.

2. Basic properties of the MPPC array

2.1. 4×4 MPPC array and setup

The large-area monolithic MPPC array described here was specifically designed and developed for future applications in

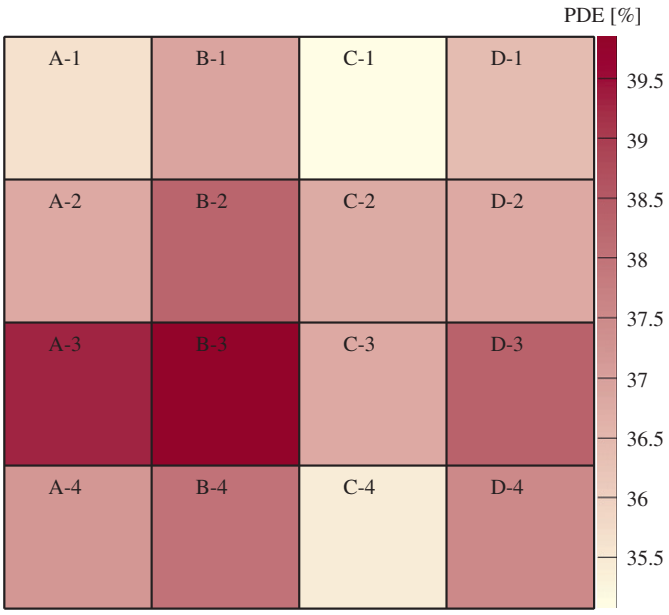

Fig. 5. PDE distribution (at an LED light wavelength of 465 nm) for all pixels at 71.9 V at 0 °C.

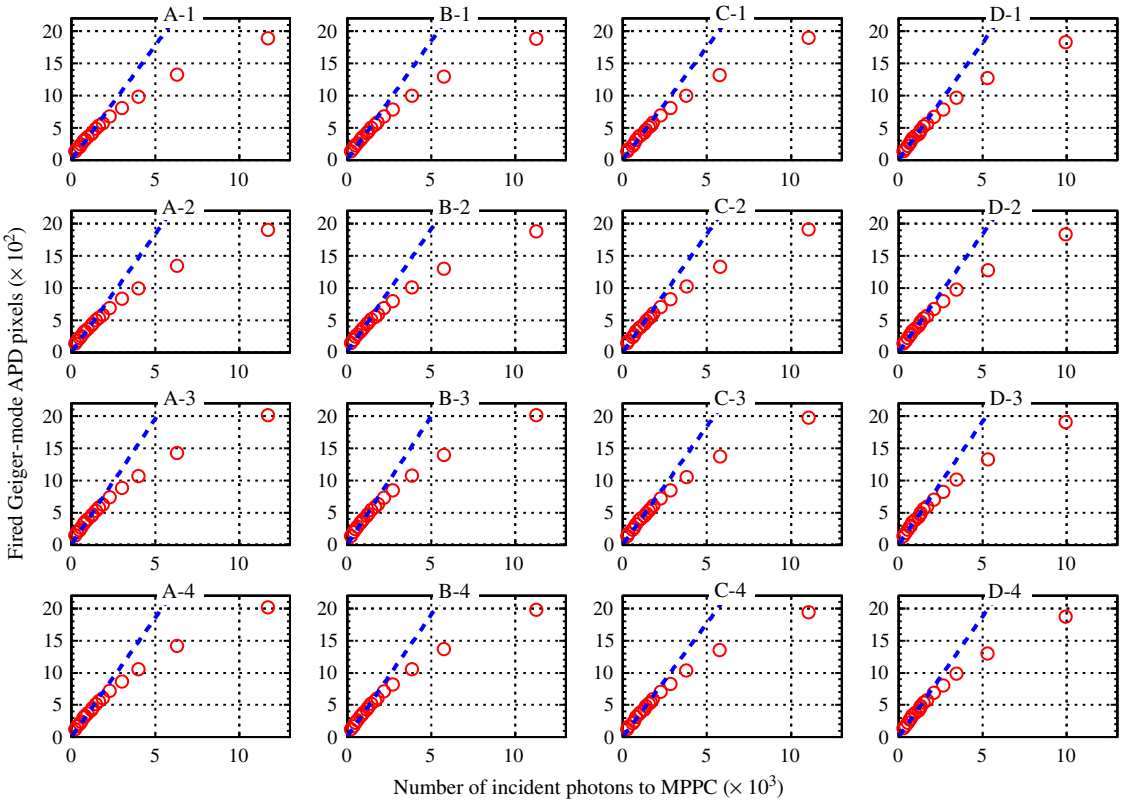

Fig. 4. Fired Geiger-mode APD pixels as a function of the number of incident photons to the MPPC, as described in the text. All data were measured at 71.9 V at 0 °C. Circles and dashed lines represent the actual measured value and the fitting line in linear region (i.e. $\leq$600 fired APD pixels), respectively.

nuclear medicine (e.g., PET scanners) by Hamamatsu Photonics K. K. The MPPC array consists of a 4×4 array of individual $3\times3\ mm^2$ pixels and a 0.2 mm gap between them. Each pixel comprises 60×60 Geiger-mode APDs arranged with a pitch of 50 μm. The dark current of each MPPC pixel ($3\times3\ mm^2$) is typically 3 μA with a gain of 7.5×10^5 measured at 25 °C. Other basic characteristics of the MPPC array are summarized in Table 1. The MPPC array tested here is placed on a printed wiring board (PWB) package measuring 25.0 by 21.0 mm and 2.7 mm thick, and using conventional epoxy resin as an entrance window to the MPPC array. Also the bonding pads are gathered at the bottom side of the device, as shown in Fig. 1 on the *left*. All 4×4 pixels have a common cathode, namely, the same positive voltage is biased at the same time, whilst signals from individual anodes can be read through the signal pins gathered at the bottom-side of the PWB (Fig. 1 *right*).

First, the gain characteristic of each 4×4 MPPC pixel was measured as a function of bias voltage. All the measurements were conducted at 0 °C to reduce the contamination of dark counts. The diagram of setup used for measuring gain is shown in Fig. 2 (*top*). The MPPC array was irradiated by the weak blue light (465 nm; close to the peak wavelength of Ce:LYSO) of a light emitting diode (LED), and the output charges from the MPPC were estimated by the single photoelectron (1 p.e.) peak, which was individually taken with charge-sensitive ADC (HOSHIN V005; hereafter CSADC). The input gate of the CSADC, 100 ns in width, was activated simultaneously when triggering the LED. The output signals from the MPPC array were amplified by a factor of 100 using the fast current amplifier (Phillips MODEL 6954).

Second, the proportionality of the output signal relative to the number of incident photons was measured for each MPPC pixel at a bias voltage of 71.9 V. The diagram of setup used for measuring the proportionality is shown in Fig. 2 (*bottom*). To calibrate the absolute number of incident LED photons entering the MPPC window, a PMT (Hamamatsu R 7899-MOD1 (EG)) was set beside the MPPC array. The output signals from both the PMT and MPPC were measured directly by the CSADC. Subsequently, the number of incident photons to the MPPC array was estimated by taking account of the various effective areas of the PMT and MPPC array as well as minor distance corrections between the LED and each of the photo-detectors. Also we assumed the quantum efficiency of the PMT to be 25% at an LED wavelength of 465 nm.

Finally, the variation of dark counts for individual MPPC pixels was measured as a function of the pulse height of output signals. The MPPC was operated with a bias voltage of 71.9 V. Output signals from the individual MPPC pixel were fed into the non-update discriminator (Technoland N-TM 405) and directly counted by visual scalers (Technoland N-OR 425).

2.2. Result

A gain characteristic as a function of bias voltage is shown in Fig. 3 (*top*). The curves generally showed good linearity between 70.9 and 71.9 V, corresponding to the measured gain of $\simeq(4-10)\times10^5$. Note that the gain curves fitted well with a slope of 5.16×10^5 gain/V, and distribution (among 4×4 pixels) of only $\pm4.0\%$. The uniformity of the gain measured at a bias voltage of

Table 2
Basic characteristics of the Ce:LYSO and Pr:LuAG scintillators.

	Ce:LYSO	Pr:LuAG
Pixel size (mm^3)	$3\times3\times10$	
Density (g/cm^3)	7.10	6.73
Light yield (photons/MeV)	25,000	20,000
Decay time (ns)	40	20
Peak wavelength (nm)	420	310

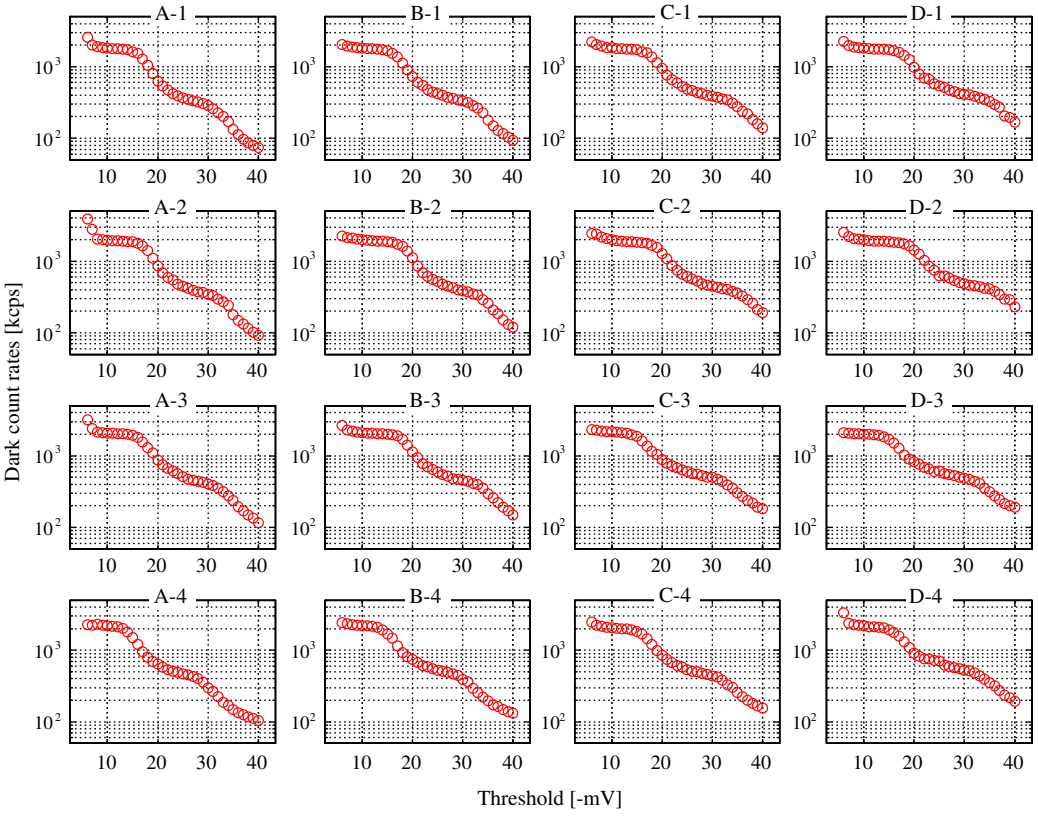

Fig. 6. Dark count rates as a function of a threshold voltage for all pixels measured at 71.9 V at 0 °C.

71.9 V is shown in Fig. 3 (*bottom*). The average gain was 9.68×10^5 and its variation was only $\pm7.2\%$ over 4×4 MPPC pixels. Note that the uniformity of the gain at a bias voltage of 71.9 V is slightly worse than that expected from the variation of the gain slope ($\pm4\%$). This is possibly due to fluctuations in the breakdown voltage caused by the uniformity of the avalanche gain within the pixels.

As shown in Fig. 4, the total number of fired Geiger-mode APD pixels does not directly correspond to the number of detected photons; each of the MPPC pixels respond almost linearly up to the 600 fired Geiger-mode APD pixels, even though the total number of pixels is 3600. To quantify the PDE, the slope of the curves was determined within this linear range (i.e. ≤600 fired APD pixels). The resultant PDE map is shown in Fig. 5. The average PDE is 37.2% (at an LED light wavelength of 465 nm), and its variation is $\pm6.4\%$ among 4×4 MPPC pixels.

The variations of the dark count rates as a function of threshold voltage for each MPPC pixel are shown in Fig. 6. It is clear that dark count rates due to 1 p.e. clearly appear as a plateau between -10 and -15 mV, and its count rate is about 2 Mcps/pixel.

3. Performances with pixelized scintillators

3.1. Scintillators and setup

In our experiments, Ce:LYSO, Pr:LuAG and Pr:LuAG (WLS) were chosen to be coupled with the MPPC array described above. The basic parameters of Ce:LYSO and Pr:LuAG are summarized in Table 2. We note that the peak wavelength of Ce:LYSO favors MPPC because the latter is sensitive within the range 350–650 nm [8]. In this sense, a UV light emission of Pr:LuAG, peaking at 310 nm, is not favorable but its short decay time (20 ns) is particularly noteworthy as implemented in future TOF-PET scanners (see Section 1) and also beneficial for MPPC to effectively reduce dark counts within a narrower coincidence window. We therefore fabricated another sample, Pr:LuAG (WLS), which was coated with a WLS layer of 20 μm that converts the 310 nm scintillation light of the Pr:LuAG to 420 nm light. The WLS comprises a solution including polyvinyl-toluene and plastic scintillators such as bis-MSB (p-bis(*o*-methylstyryl) benzene) and TV-PVD (2-(4-terbutylphenyl)-5-(4-biphenyl)-oxadiazol-1,3,4) [19]. These scintillator matrices were fabricated to have geometries precisely matching the MPPC array, namely, a 4×4 array of $3\times3\times10$ mm^3 pixels, and a 0.2 mm gap between them. Each scintillator pixel is divided with a reflective $BaSO_4$ layer of 0.2 mm thickness. Fig. 7 shows a picture of the 4×4 matrices consisting of Ce:LYSO (*right*), Pr:LuAG (*center*) and Pr:LuAG (WLS) (*right*), respectively. Silicon optical grease (OKEN N6262A) was used for optical coupling between the scintillator matrices and the surface of the MPPC array.

The performance of the MPPC array coupled with these pixelized scintillators was evaluated by taking the energy spectra of a ^{137}Cs source. All data were taken at 71.9 V at 0 °C. The diagram of setup used for measuring energy spectra is shown in Fig. 8. The output signals from each MPPC pixel were divided by a Quad Linear FAN IN/OUT (Phillips MODEL 6954) and then sent to the CSADC after a 100 ns delay, to ensure appropriate timing against the input gate signal (also activated from the same anode signal). We set gate widths of 300 ns for the Ce:LYSO and 250 ns for the Pr:LuAG and Pr:LuAG (WLS), respectively. The threshold voltage of the signals was set at around 60 p.e.

3.2. Result

When the MPPC array is coupled with the Ce:LYSO matrix, the output charge for 662 keV gamma-rays is approximately 308 pC,

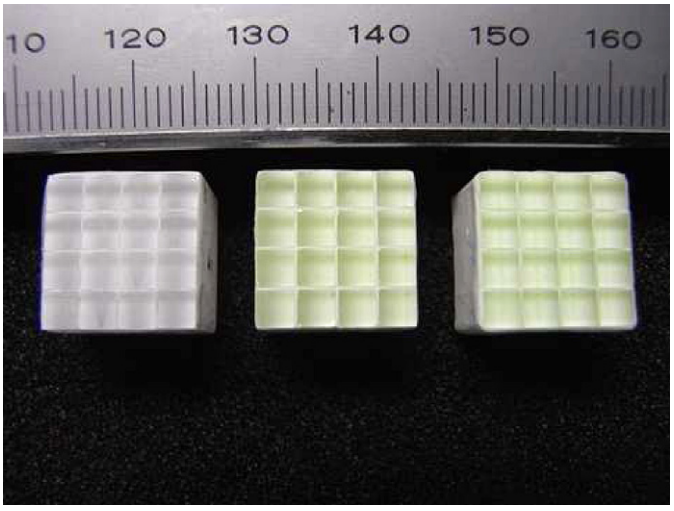

Fig. 7. Pictures of the 4×4 scintillator matrices to be coupled with the MPPC array. (From *left* to *right*: Ce:LYSO, Pr:LuAG, Pr:LuAG (WLS)).

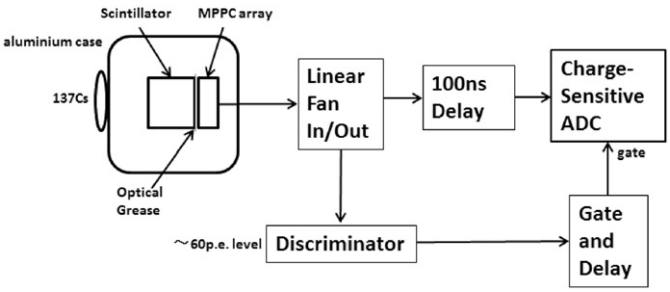

Fig. 8. Diagram of the readout system used for measuring energy spectra.

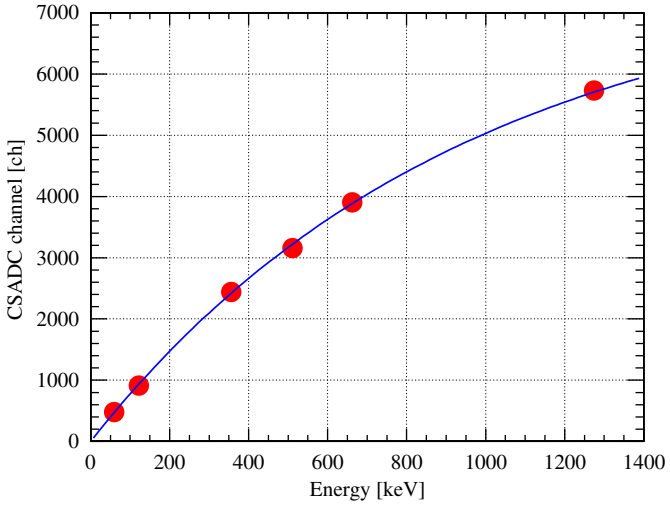

Fig. 9. An example calibration curve of the CSADC channel versus gamma-ray energy for a pixel A-1 with Ce:LYSO. Circles and line represent the actual measured value and fitting function, respectively. From left to right circle, ^{241}Am, ^{57}Co, ^{133}Ba, ^{22}Na, ^{137}Cs, and ^{22}Na sources were used.

which corresponds to $\simeq2150$ fired Geiger-mode APD pixels. Apparently such abundant incident photons will cause substantial non-linearity in the MPPC response, as already seen in Fig. 4. To calibrate the energy and output ADC channel (i.e. charge) relation of the CSADC, the proper functional dependence was initially measured for the Ce:LYSO crystal using various gamma-ray

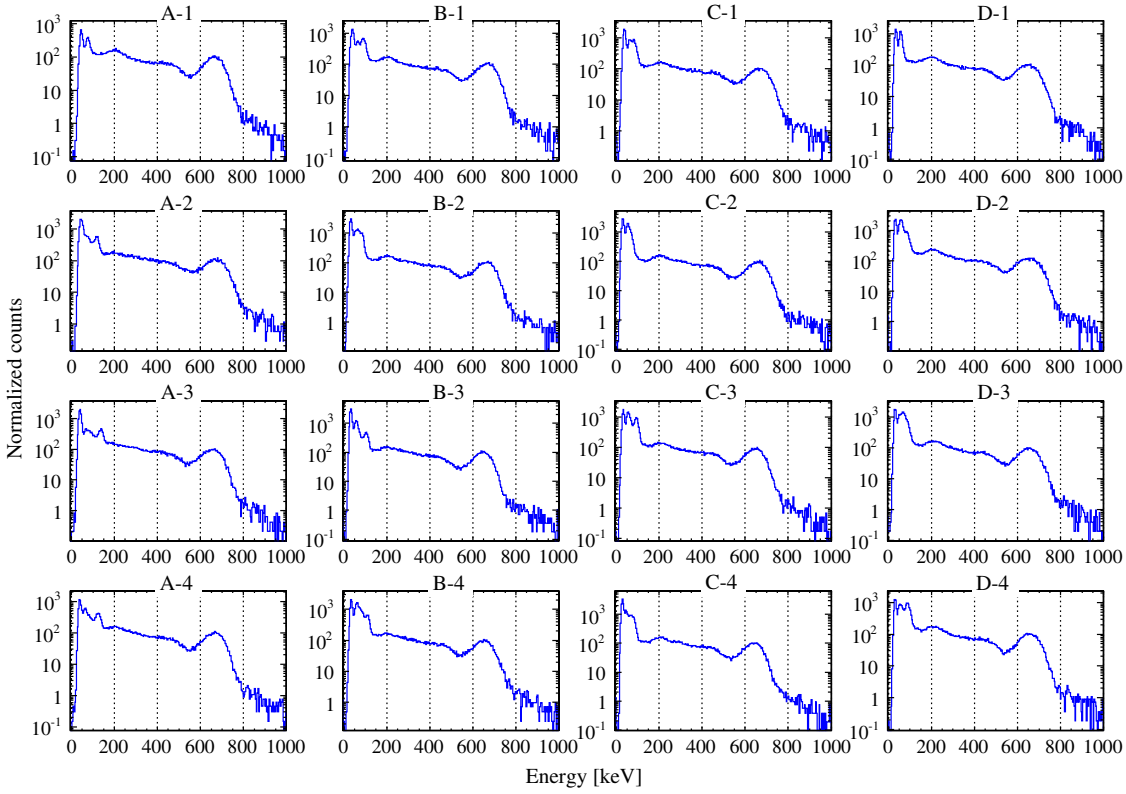

Fig. 10. Energy spectra of a ^{137}Cs source coupled with the Ce:LYSO matrices on the MPPC array for all pixels at 71.9 V at 0 °C.

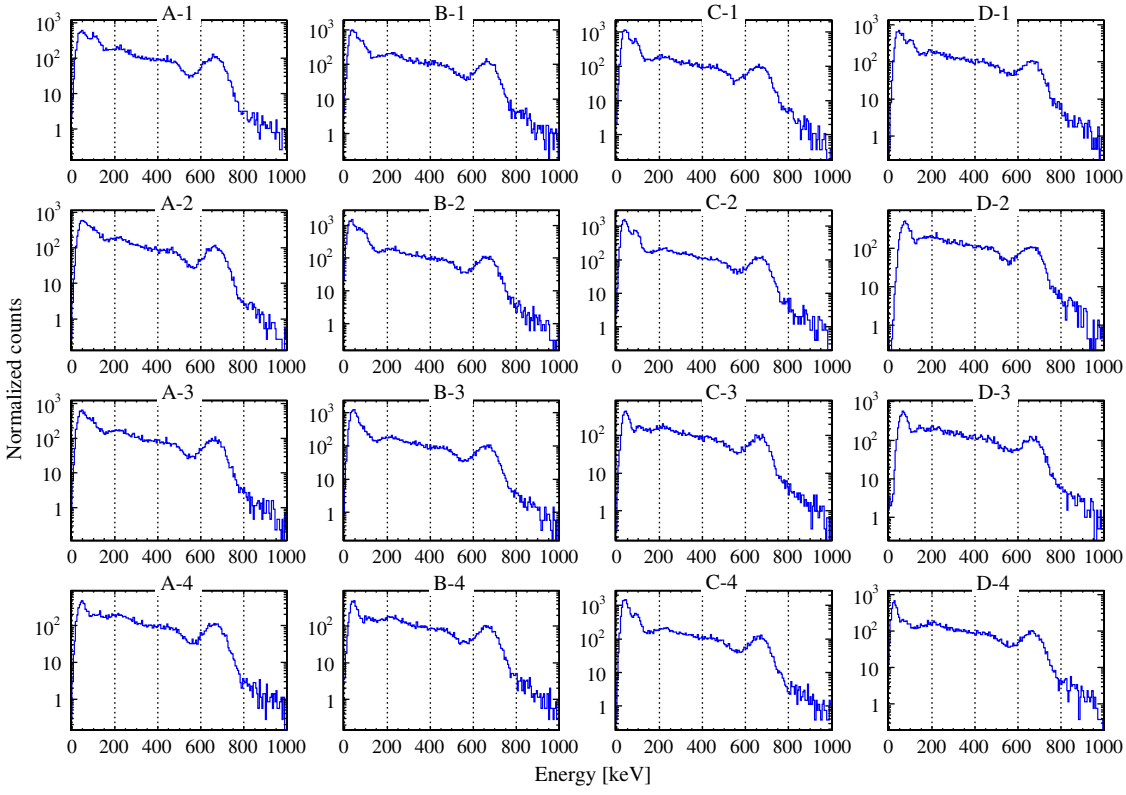

Fig. 11. Energy spectra of a ^{137}Cs source coupled with the Pr:LuAG matrices on the MPPC array for all pixels at 71.9 V at 0 °C.

sources, ^{22}Na, ^{57}Co,^{133}Ba, and ^{241}Am for each MPPC pixel. The results are shown in Fig. 9. As discussed in detail in literature (e.g., Ref. [20]), the relation is well represented by a simple function of the form

$$ADC[\mathrm{ch}] = a \times \{1-\exp(-bE(\mathrm{keV})/a)\} \quad (1)$$

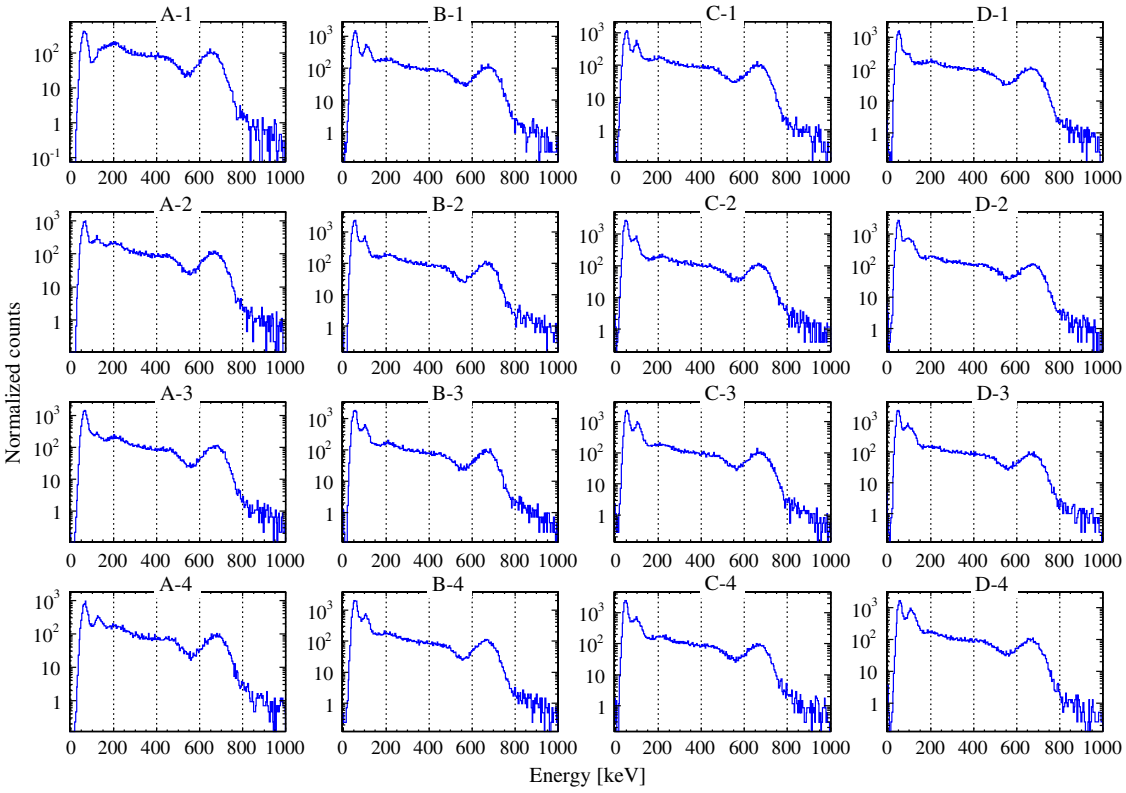

Fig. 12. Energy spectra of a ^{137}Cs source coupled with the Pr:LuAG (WLS) matrices on the MPPC array for all pixels at 71.9 V at 0 °C.

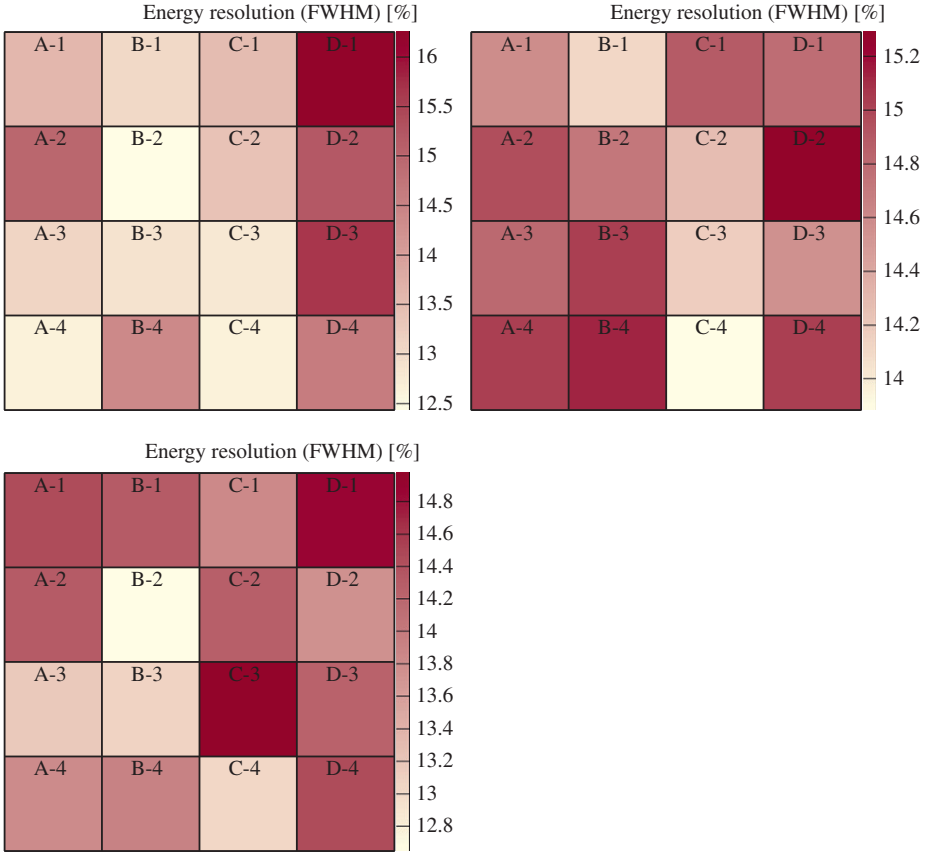

Fig. 13. Variation of energy resolution for 662 keV gamma-rays measured with the MPPC array and the various scintillators, the Ce:LYSO (*top left*), the Pr:LuAG (*top right*) and the Pr:LuAG (WLS) (*bottom*).

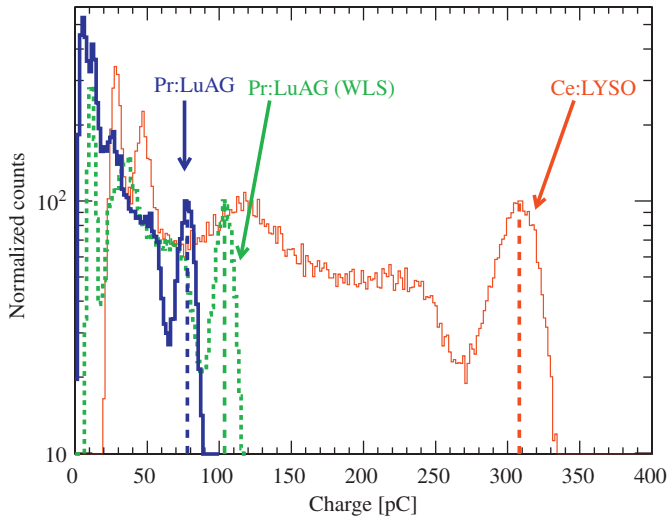

Fig. 14. Comparison of the charge amount from one of the MPPC array pixels (pixel A-1) coupled with the three scintillator matrices (Ce:LYSO, Pr:LuAG and Pr:LuAG (WLS)). The solid, thick solid and dashed lines represent the spectra of a ^{137}Cs source with Ce:LYSO, Pr:LuAG and Pr:LuAG (WLS), respectively.

where *ADC* [ch] is a measured channel of the CSADC, *E* (keV) is the energy of the gamma-ray sources, and *a*,*b* are fitting constants. Similarly, for the case of the Pr:LuAG or Pr:LuAG (WLS) matrix, the 662 keV photoelectric peak corresponds to about 530 or 760 fired Geiger-mode APD pixels, respectively. Therefore, the MPPC array with a Pr:LuAG matrix is operated well within the linear range, whilst the data taken with the Pr:LuAG (WLS) are marginally affected by the non-linear response. Therefore, a calibration equivalent to that applied for the Ce:LYSO matrix was also used to fix the response of the Pr:LuAG (WLS) matrix.

The energy spectra measured with ^{137}Cs corrected for non-linearity are shown in Figs. 10 (Ce:LYSO), 11 (Pr:LuAG) and 12 (Pr:LuAG (WLS)). The average values of energy resolutions for the 662 keV photoelectric peak measured with Ce:LYSO, Pr:LuAG, and Pr:LuAG (WLS) matrices were 13.83%, 14.70%, and 13.96% (FWHM), respectively. The energy resolution variations among 4×4 pixels were $\pm12.5\%$, $\pm4.8\%$, and $\pm8.4\%$, respectively, as shown in Fig. 13. Finally, a direct comparison of output charges from the MPPC array was made for different scintillators in Fig. 14, corrected for non-linearity. It was clear that the output charge from the MPPC array with the Pr:LuAG (WLS) matrix was about 30% larger than that of the Pr:LuAG matrix, as expected from the improvement of PDE between 310 and 420 nm.

4. Conclusion

In this paper, the initial performances of the large-area monolithic 4×4 MPPC array of 3×3 mm^2 pixels newly developed by Hamamatsu Photonics K. K. were reported. Excellent uniformities of $\pm7.2\%$ and $\pm6.4\%$ were obtained for gain variations and PDE distribution, respectively, as measured at 0 °C. The dark count rates were also measured to 2 Mcps. Next, 4×4 Ce:LYSO, Pr:LuAG, and Pr:LuAG (WLS) matrices of individual $3\times3\times10$ mm^3 scintillator crystals were fabricated as a sensor head of a compact gamma-ray camera. An average energy resolution of 13.83% (FWHM) was obtained with the Ce:LYSO matrix, as opposed to 14.70% (FWHM) and 13.96% (FWHM) with the Pr:LuAG and Pr:LuAG (WLS) matrices, respectively. The output charges for 662 keV gamma-rays, corrected for non-linearity, were 308, 77 and 104 pC, respectively, as measured with one of the MPPC pixels (pixel A-1) coupled with a Ce:LYSO, Pr:LuAG, and Pr:LuAG (WLS) pixel. These results indicate that a large-area monolithic MPPC array coupled with a Ce:LYSO or Pr:LuAG matrix could be a useful device for medical imaging.

Acknowledgment

We thank an anonymous referee for his/her useful comments and suggestions to improve the manuscript.

References

[1] W.W. Moses, Nucl. Instr. and Meth. A 471 (2001) 209.
[2] J. Malamitsi, et al., Nucl. Instr. and Meth. A 569 (2006) 319.
[3] R.R. Raylman, et al., Nucl. Instr. and Meth. A 569 (2006) 306.
[4] J.E. Mackewn, et al., in: IEEE Trans. Nucl. Sci. Conference Record, vol. M09-248, 2009, p. 3307.
[5] H. Peng, et al., Nucl. Instr. and Meth. A 612 (2010) 412.
[6] C. Woody, et al., Nucl. Instr. and Meth. A 571 (2007) 102.
[7] J. Kataoka, et al., IEEE Trans. Nucl. Sci. NS-57 (5) (2010) 2448.
[8] K. Yamamoto, et al., in: IEEE Trans. Nucl. Sci. Conference Record, vol. N30-102, 2006, p. 1094.
[9] K. Yamamoto, et al., in: IEEE Trans. Nucl. Sci. Conference Record, vol. N24-292, 2007, p. 1511.
[10] A. Braem, et al., Nucl. Instr. and Meth. A 586 (2008) 300.
[11] C.L. Kim, et al., IEEE Trans. Nucl. Sci. NS-56 (5) (2009) 2580.
[12] S. España, et al., Nucl. Instr. and Meth. A 613 (2010) 308.
[13] A. Nassalski, et al., IEEE Trans. Nucl. Sci. NS-57 (3) (2010) 1008.
[14] H. Alva-Sánchez, et al., Nucl. Instr. and Meth. A 604 (2009) 335.
[15] M. Conti, et al., IEEE Trans. Nucl. Sci. NS-56 (3) (2009) 926.
[16] K. Kamada, et al., IEEE Trans. Nucl. Sci. NS-56 (3) (2009) 570.
[17] M. Yoshino, J. Kataoka, T. Nakamori, H. Matsuda, T. Miura, Y. Ishikawa, N. Kawabata, Y. Matsunaga, K. kamada, Y. Usuki, A. Yoshikawa, T. Yanagida, Development and performance of UV enhanced APD-arrays for high resolution PET imaging coupled with pixelized Pr:LuAG crystal, Nucl. Instr. and Meth. A, submitted for publication.
[18] C.L. Kim, et al., in: IEEE Trans. Nucl. Sci. Conference Record, vol. M05-73, 2009, p. 2636.
[19] K. Kamada, T. Yanagida, T. Endo, Y. Fujimoto, Y. Usuki, A. Yoshikawa, Read out test of inorganic-organic hybrid scintillator; Pr:LuAG single crystal covered with plastic scintillator, IEEE Trans. Nucl. Conference Record, A, submitted for publication.
[20] M. Szawlowski, et al., in: IEEE Trans. Nucl. Sci. Conference Record, vol. NM1-5, 2007, p. 4591.